SPACE TELESCOPE SCIENCE INSTITUTE

ORBITAL FOCUS VARIATIONS IN THE HUBBLE SPACE TELESCOPE

by Pierre Y. Bély, Hashima Hasan and Manfred Miebach

Space Telescope Science Institute, Baltimore, MD 21218

Abstract

1. Introduction

Soon after the start of observations with the Hubble Space Telescope (HST), evidence was found of the instability of the focus of the telescope on a time scale on the orbit (Figure xx). Although small, this effect was very noticeable because of the spreading of the images caused by spherical aberration in the HST primary mirror. When blinking images of the same object taken at different times along the orbit, the focus instability manifested itself as a radial expansion or contraction of the point spread function (PSF), and was dubbed "breathing". The effect was rapidly identified as resulting from a short term focus change, and was crudely characterized after a dedicated observation test. Efforts to relate the phenomenon to the telescope environment have been partially successful. While we now know that HST breathing is thermally driven, a full understanding of the thermal effect is still under study.

We report here on the characteristics of the phenomenon and its effect on image quality, flux density measurements and telescope guiding. The test conducted to characterize breathing is discussed in section 1. An empirical model relating short term focus changes to HST light shield temperatures is described in section 2, while the effect of breathing on observations with the repaired HST is discussed in section 3.

2. Dedicated test for phenomenon characterization

2.1 Test description

A dedicated test was executed on day 1993.145 using the the two HST cameras, the Wide Field Planetary Camera (WFPC) and the Faint Object camera (FOC), in parallel. The basic idea was to take as many exposures as possible of a point source with an optimum signal/noise ratio, for two orbits. In order to investigate a possible thermal dependence of the phenomenon, one series of observations was taken in the "hot attitude" where the spacecraft offers its largest cross section to the sun (in the CVZ) and another series in the "cold attitude" where the spacecraft is pointing away from the sun, and its cross section facing the sun is minimal. The first series allowed continuous observation of the target over a full orbit, while the second, with the target roughly in the orbital plane, suffered from earth occultation so that data could be taken only over roughly half of the orbit. The reason for using the two cameras was to increase the amount of data points collected and ensure that there was no instrument specific contributions. In addition to the cameras, the third Fine Guidance Sensor (FGS) was used in astrometry mode to detect any change in the guide star centroiding which could result from the focus changes.

The primary instrument was the FOC f/96 in small (256 x 256) format, since it is the instrument with the highest spatial resolution on the telescope. The star was a bright star, xxxx (magnitude) exposed over xxx in order to give about 25 counts/pixel/second in the rings structure of the PSF, even at the expense of saturating the core.

Planetary Camera (PC) exposures were taken in parallel in as large a number as allowed by the storage capacity of the tape recorder. A total of 10 FOC and 44 PC exposures were taken for the hot attitude and 6 FOC and 28 PC exposures for the cold attitude. The FOC exposures were 300 seconds long while those for the PC were 20 seconds.

2.2 Analysis of the test results

The two methods which have been traditionally used for the determination of HST focus are the phase retrieval method and the pad method (*References ???*). The phase retrieval method determines the wavefront errors in the image by fitting the data to a theoretical model point spread function. The pad method exploits the fact that well exposed spherically aberrated stellar images taken with HST have images of the pads supporting the HST primary mirror, clearly visible. The distances from the image center of the pads visible in the image are related to the distance of the position of the HST secondary mirror from its position at paraxial focus. Both methods give absolute values for the focus error. Another method has also been developed (Baxter et al., 1993) for measuring focus changes between two FOC images called the "ring" method. The ring method is empirical and relates the shift in ring positions in the azimuthally averaged PSF profile to focus shifts. The assumption is that the shift in the rings is due only to a focus change.

For most applications the methods works well. However, if there is too much noise or jitter in the images the fitting procedure does not give a good convergence. The pad method, by virtue of its simplicity, has been the preferred one for routine focus monitoring. The main drawbacks of this method are that it is subjective and the reproducibility of the values of the secondary mirror displacement obtained by repeated measurements of the pad centers in a single FOC image is ± 3 microns. The method is adequate for focus monitoring but is not so good for measuring the "breathing" effect which is fairly small.

The three methods have been used in the analysis of the test data and are in excellent agreement. Since the phase retrieval method is the most rigorous of the three methods, and in addition to values of the focus error gives those for other wavefront aberrations as well, the results presented here are based on this method only.

In the phase retrieval method a theoretical model of the PSF is fitted to the data. Using standard Fourier techniques the PSF is expressed in terms of Zernike coefficients which represent different optical distortions (Seidel aberration) of the system. The expansion coefficients give the "strength" of the aberration.

We minimize a merit function which is the RMS difference between a simulated and observed PSF, using a non - linear fitting routine CURFIT (Bevington, 1969) by varying the aberration coefficients. This method allows an independent estimate of spherical aberration and focus, unlike the pad method which gives focus for an assumed amount of spherical aberration.

The aberration coefficient Z_4 represents the departure from diffraction focus (caused by spherical aberration) and can be shown by geometric arguments to correspond to a secondary mirror displacement, $\Delta(SM)$ by

$$\Delta(SM) = (Z_4^c - Z_4^p)(3.887 \times 8F^2)/110$$

where $\Delta(SM)$ is expressed in microns as before, Z_4^c and Z_4^p are the values at the focus position being measured and paraxial focus respectively, and $F = 24 \times 0.9984$ is the actual image space focal ratio at paraxial focus. At paraxial focus the wavefront error is proportional to r^4. Thus Z_4^p may be easily computed by equating the r^2 term in the orthogonal expansion of spherical aberration to the r^2 term from the focus polynomial with coefficient Z_4. For the HST we get $Z_4^p = -1.249$ microns.

The measurements were expressed in secondary mirror motion along the optical axis, with reference to xxxxx

2.3 Results

The two sets of focus measurements (CVZ target and in-plane or ecliptic target) are plotted with reference to the first exposure in each set in Figure 1. A comparison of the two sets indicate that the ecliptic sequence should be shifted up by 2 microns (±0.5 micron) with respect to the CVZ set.

Detailed inspection of the data suggests a strong correlation with the orbital thermal state of the spacecraft as opposed to the other thermal radiation sources such as the bright earth albedo, or even other driving mechanisms such magnetic field or gravity gradient. After trying various parameters we find that quite good a correlation is obtained when using the temperature of the portion of the light shield directly in front of the secondary mirror (Sensors T307 to T310 at station 494 - see Figure 2).

The empirical relation found is given by

$$SM = 0.7(LS - MLS) + 0.4$$

where LS is the mean of the 4 light shield temperature sensors mentioned above, MLS is the running orbital average of LS (i.e. over the previous 96 minutes) and SM is the secondary mirror motion in microns. As shown in Figure 3, where focus data is plotted against this model, the agreement is quite good. The fact that the effect seems induced by the *relative* orbital temperature swing in the light shield and is not sensitive to *absolute* value of the temperature is probably the result of differential or "bi-metallic" type of effect, as opposed to pure expansion effect. In other words the effect could be due to a temperature sensitive element the bulk temperature of which is at an *orbital average*,****** but which skin is sensing the *current* environment*******??.

3. Validation of the focus model

The focus model is tested against documented cases of short term focus change experienced by the FOC and the WFPC and a few cases of short term flux variation seen in the other science instruments (SI) which could be attributed to *either* an image drift or a focus change, or both.

Fig shows the Doradus phase retrieval plotted vs temperature data

Fig xx shows the focus monitor data – Individual test do not provide enough data , but statistically we find a trend (focusmonitor.pro)

Before the repair mission of December 1993, images suffered from spherical aberration with a spread which could be comparable to the sizes of the photometer and spectrograph apertures, and could result in flux variation on an orbital time scale. This effect was first noticed on a long exposure with the High Speed Photometer (Proposal 1389 on day 91.234 with a 1 arcsecond aperture), which showed a clear orbital flux variation combined with a linear trend. To verify quantitatively the effect, we use direct photometry measurements of the the FOC exposures obtained in the breathing test, and find that one micron of secondary mirror displacement induces a change of 0.78 percent in the flux within 1 arcsecond.

Combining this result with the breathing formula above gives the following flux change equation (for a 1 arcsecond aperture, and neglecting the effects of astigmatism in off-axis apertures):

$$\Delta\Phi = .0078 * 0.7 * (LS - MLS)$$

a formula which fits the data very well as shown on Figure 4.

4. Effect on observations with the repaired HST

The orbital focus changes can affect the quality of the science data in many ways. The most obvious effect is loss in sensitivity resulting from image blur. However, there are many other ramifications such as the difficulty in performing image enhancement with an unstable PSF, or the impossibility of doing photometry with the cameras or the spectrographs. There are also secondary effects due to the focal plane shifts induced by the FGS reacting to focus variation (when guiding in fine lock).

These effects can be very subtle and certainly depend on the type of observation done (limiting detection, crowded fields, etc...), and complex simulations may be required in order to pinpoint the level at which focus change becomes intolerable.

With spherical aberration corrected, it is now much more difficult to measure the effect of focus change on the instrument data. To evaluate the importance of these effects, we have performed simulations to determine the variation of the PSF at various wavelengths and in the various instruments.

The PSF have been determined using the Telescope and Instrument Modelling (TIM) software, with the mirror wavefront errors (excluding spherical aberration) as measured pre-launch and a $\lambda/40$ wavefront for the rest of the optics (secondary mirror residual misalignment, COSTAR and FOC/FOS/GHRS or WFPC II internal wavefront errors.

The results of our calculations are shown in the attached figures. Figure 5 gives the Strehl ratio vs focus as a function of wavelength, for the two cameras, and Figure 6 and 7 the energy ensquared in a 0.25×0.25 and 1×1 arcsecond apertures respectively. The focus error is expressed in term of secondary mirror despace.

We should revise the following text to determine the effect knowing the max amplitude of secondary mirror motion

Figure gives the tolerable focus error for the cameras as a function of wavelength (using the 20 % Strehl ratio degradation criterion), and Figures 8 the tolerable focus error for the spectrographs. In the case of the spectrographs, the small aperture criterion is the only driver, the 1% degradation for the large aperture being always met even for very large focus errors.

As expected, the most stringent focus requirement is set by the cameras. For them, the focus should not change by more than ±3 microns when working in the far UV, and by not more than ±5 microns in the visible. The tolerance for the spectrographs is much wider, about ±10 microns.

Actual data:

omegacen post sm (fig done on Jan 3 96)

FOC – Manfred to do

Safe mode entry – long stay a cold temperature: what do we say?

5. Effect on telescope guiding

Separation between guide stars

Change on position in FGS (10 mas)

6. References

B axter D., Greenfield P. E., Hack W., Nota A., Jedrzejewski R. I. and Paresce F., 1993 *STSCI preprint series* No. 751.

B urrows C., 1990 *OTA Handbook.*

H asan H., 1992 *STSCI Newsletter* vol. 9, no. 2, p 17.

H asan H., Burrows C. and Schroeder D., 1993 *PASP* October issue and *Instrument Science Report* OTA-12.

Figure 1. Doradus (2 images)

Figure 1. Breathing test data

Figure 2. Sketch of HST with sensors

Figure 3. Secondary mirror motion derived from analysis of images were taken both with the PC and the Faint Object Camera (FOC) of stars in the ecliptic plane as well as in the CVZ, over two orbits. Agreement of the data with the breathing curve, shown by the solid line, is excellent.

Figure 4. Hsp data

Figure 4. Strehl ratio vs. focus at five wavelengths for the cameras. The Strehl ratio degrades more rapidly in the UV than in the visible. However, since WFPC2 is not designed to give optimal imaging in the UV, the Strehl ratio degradation criterion is not as important in the UV as in the visible.

Figure 1. Typical focus time variation in the WFPC2 over a 3 orbit period. The predicted focus change, shown in solid line, was around 8 micron peak to peak. The actual focus data obtained from phase retrieval has a lot of scatter (point symbols different for each camera) and does not exhibit a particular trend. The data between each cameras do not strongly agree even when adjusting the focus offset. This suggests that the focus variations are mostly due to errors in the phase retrieval measurements and not to breathing. (Data taken period in june 1994, on a omega-cen – bright star – best we can do for phase retrieval) .

UNUSED CAPTIONS

Figure 5. Ensquared energy in 0.25" × 0.25" aperture in spectrographs vs. focus position. Throughput through this aperture degrades slowly with defocus for all wavelengths.

Figure 6. Ensquared energy in 1" × 1" aperture in spectrographs vs. focus position. Dependence of throughput through this aperture on defocus is negligible for all wavelengths.

Figure 7. Tolerable focus error for the cameras as a function of wavelength (using the 20% Strehl ratio degradation criterion.) The SM despace plotted here represents the peak to peak variation of the focus relative to the best focus. In the UV the tolerance for the FOC is ±1.8 microns of SM movement, while the PC2 can withstand ±3 microns. In the visible, on the other hand, the FOC can tolerate ±6 micron SM movement, while the tolerance for the FOC is ±4.5 microns.

Figure 8. Tolerable focus error for the spectrographs. The small aperture criterion is the only driver. The 1% degradation for the large apertures is met even for very large focus errors. The SM despace plotted here represents the peak to peak variation of the focus relative to the best focus.

Figure 9. Variation of radius encircling 80% energy with focus. An increase in radius of $\sim 10\%$ takes place for SM movements of ±5 microns.

Figure 10. Variation of the sharpness criterion defined as $\sum_i P_i^2/(\sum P_i)^2$ where P_i is the intensity in pixel i, with focus. The sharpness degrades more rapidly in the UV than in the visible, corresponding to an increas in exposure time of $\sim 4\%$ in the UV and $\sim 35\%$ in th visible.

Figure 1. 34 Planetary Camera (PC) images were taken of a star in the continuous viewing zone (CVZ) over five and a half orbits on December 25, 1992, almost half of which were taken in coarse track and the remainder in fine lock. Secondary mirror positions were deduced by phase retrieval of the images. The solid curve is the breathing equation (1). The fit to the data in fine lock is impressive. The data in coarse track was not well suited for analysis by phase retrieval because it has too much noise.

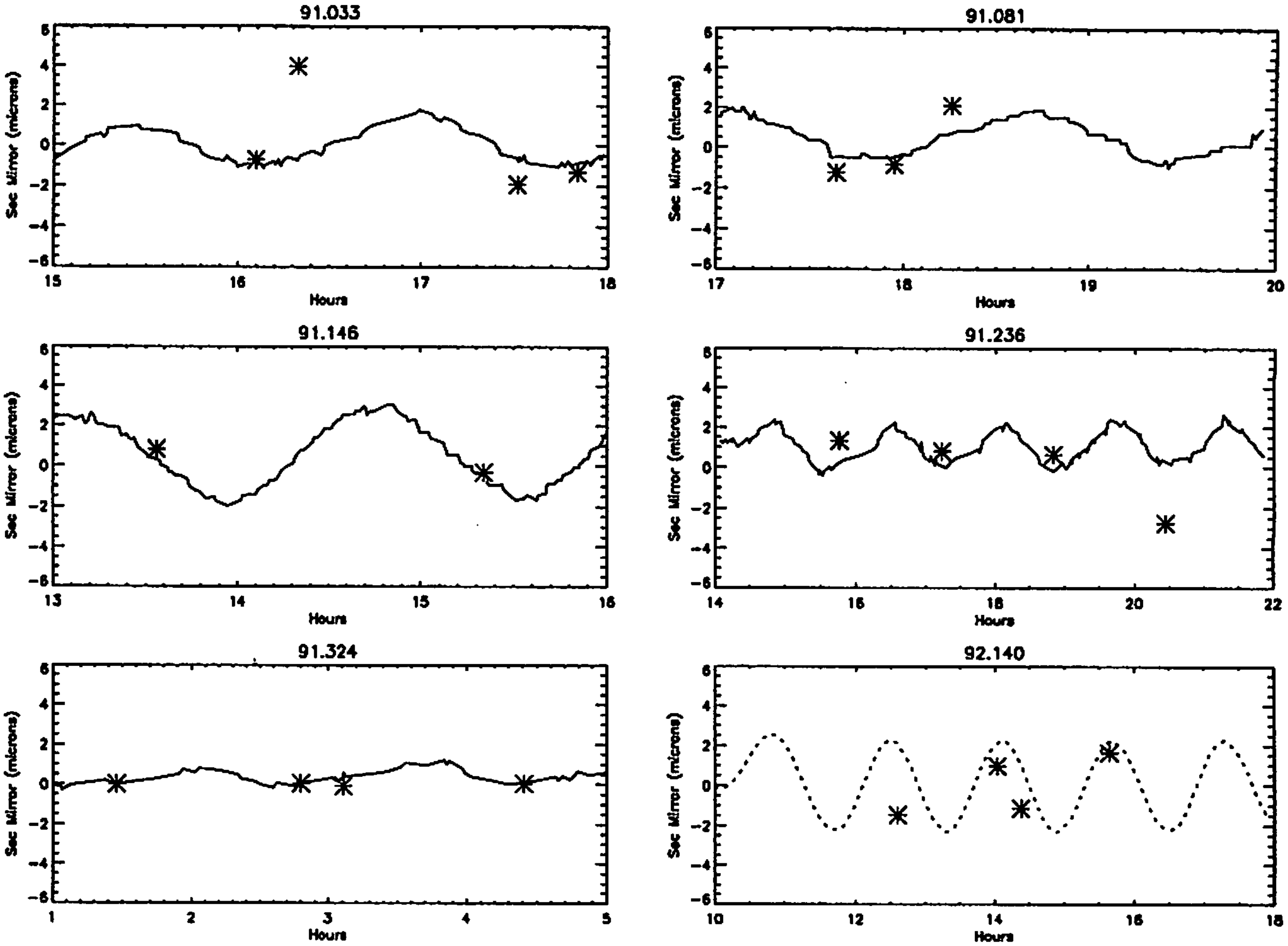
91.033
91.081
91.146
91.236
91.324
92.140
Sec Mirror (microns)
Hours

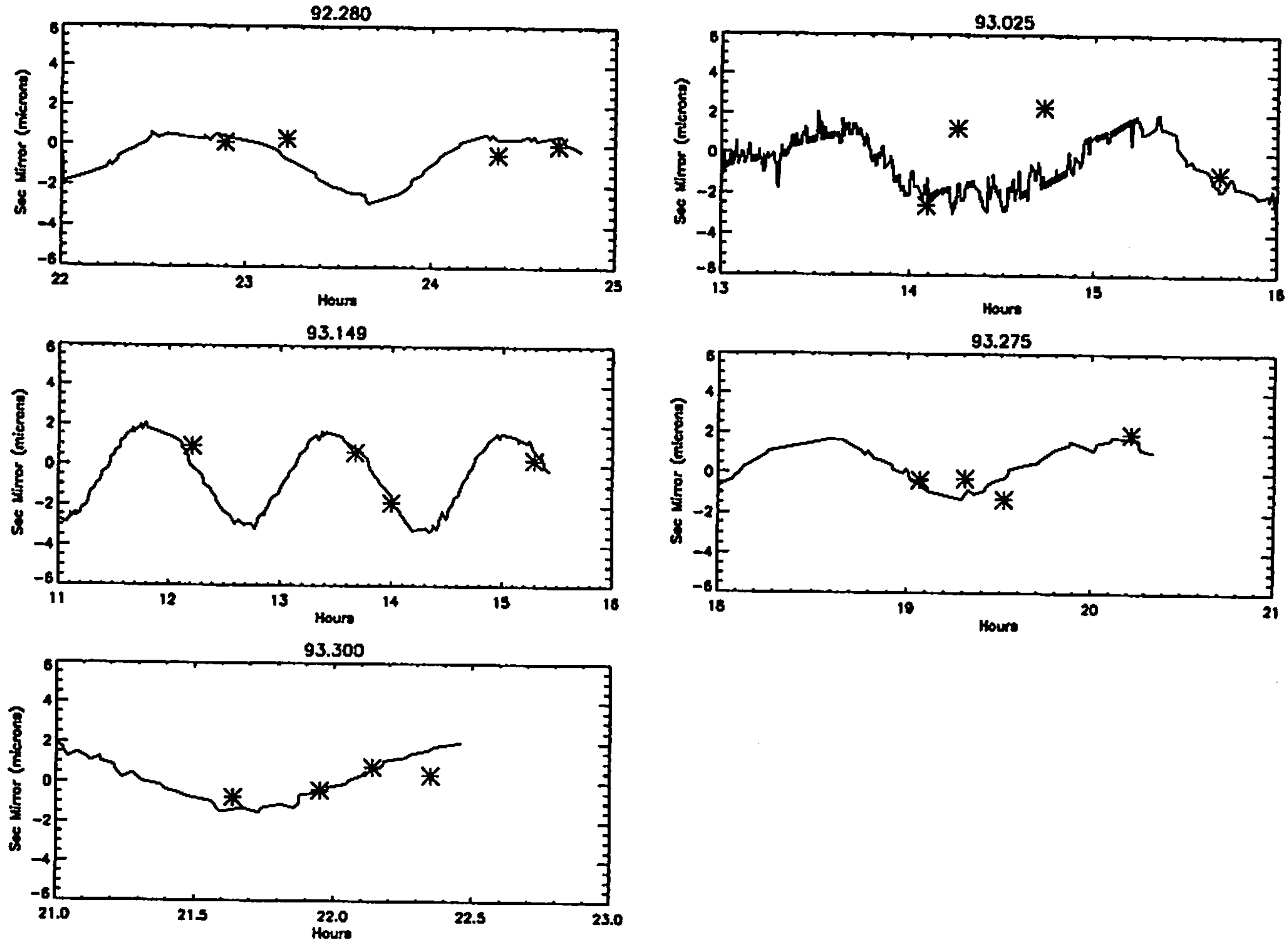
92.280
Sec Mirror (microns)
Hours
93.025
Sec Mirror (microns)
Hours
93.149
Sec Mirror (microns)
Hours
93.275
Sec Mirror (microns)
Hours
93.300
Sec Mirror (microns)
Hours